

Influence of Lithium Ions on the Ion-coordinating Ruthenium Sensitizers for Nanocrystalline Dye-sensitized Solar Cells[†]

Nara Cho, Chi-Woo Lee, Dae Won Cho, Sang Ook Kang, Jaejung Ko,* and Mohammad K. Nazeeruddin[‡]

Department of Advanced Material Chemistry, Korea University, Jochiwon, Chungnam 339-700, Korea *E-mail: jko@korea.ac.kr

[‡]Laboratory for Photonics and Interfaces, Swiss Federal Institute of Technology, CH 1015, Lausanne, Switzerland

Received January 5, 2011, Accepted May 30, 2011

Ion-coordinating ruthenium complexes [*cis*-Ru(dcbpy)(L)(NCS)₂, where dcbpy is 4,4'-dicarboxylic acid-2,2'-bipyridine and **L** is 1,4,7,10-tetraoxa-13-azacyclopentadecane, **JK-121**, or bis(2-(2-methoxy-ethoxy)ethyl) amine, **JK-122**] have been synthesized and characterized using ¹H NMR, Fourier transform IR, UV/vis spectroscopy, and cyclic voltammetry. The effect of Li⁺ in the electrolyte on the photovoltaic performance was investigated. With the stepwise addition of Li⁺ to a liquid electrolyte, the device shows significant increase in the photo-current density, but a small decrease in the open circuit voltage. The solar cell with a hole conductor, the addition of Li⁺ resulted in a 30% improvement in efficiency. The **JK-121** sensitized cells in the liquid and solid-state electrolyte give power conversion efficiencies of 6.95% and 2.59%, respectively, under the simulated sunlight.

Key Words : Dye, Dye-sensitized solar cell, Ruthenium sensitizer, Lithium cation coordination

Introduction

Environmental issues such as fossil fuel shortage and global warming have led to a greater attention on clean renewable energy during the last years. For this purpose, dye-sensitized solar cells (DSSCs) have received a great deal of attention as low-cost devices for conventional p-n junction solar cell¹. Some polypyridyl ruthenium sensitizers² have achieved power conversion efficiencies over 11% in standard air mass 1.5 sunlight. However, the efficiency of DSSCs needs to be more improved in order to become competitive with silicon-based photovoltaic cells. One of the possible approaches to increase the efficiency lies in diminishing the charge recombination by interface engineering of a dye-absorbed TiO₂, which is the main loss mechanism in competition with charge transport processes. The efficient operation of the DSSC device relies on the minimization of the possible recombination pathways occurring at the TiO₂/dye/electrolyte interface. The strategy to reduce such losses involves the coating of inorganic barrier layers³, self-assembled molecular dipoles⁴, saccharides⁵, metal-assembling dendrimers⁶, the introduction of long alkyl chains onto the dyes⁷, and the addition of co-grafting additives to the TiO₂ surface⁸. Recently, an alternative approach has addressed where the addition of Li⁺ to photoanode functions as an active device layer altering the dipole field at the interfacial region⁹. Several groups have investigated novel ruthenium sensitizers and ion-solvating supramolecular arylamines by tethering the triethylene oxide methyl ether (TEOME) to introduce ion coordinating properties to the compounds¹⁰⁻¹⁶. Lithium ion tethered by the TEOME group has been

demonstrated to retard the recombination by screening the electrons in the TiO₂ from I₃⁻. Such approach has been found to be very effective in controlling the interfacial recombination processes. However, the weak coordinating power of such a flexible TEOME unit to the lithium ion prevented the exact role of Li⁺ to the retardation of interfacial charge recombination.

In this paper we extend our studies to another alternative solubilization strategy based upon the introduction of 1,4,7,10-tetraoxa-13-azacyclopentadecane (**L1**)¹⁷ and bis(2-(2-methoxyethoxy)ethyl)-amine (**L2**)¹⁸ side groups to the 4,4'-position of a 2,2'-bipyridine ligand in order to coordinate the lithium ion strongly, as illustrated in Fig. 1 and control charge transfer at the dye sensitized nanocrystalline TiO₂/organic semiconductor heterojunction.

Experimental Section

General Methods. All reactions were carried out under an argon atmosphere. Solvents were distilled from appropriate reagents. All reagents were purchased from Sigma-Aldrich, TCI, Acros Organics and Samchun chemicals. 4,4'-Bis(4-(1,4,7,10-tetraoxa-13-azacyclopentadecan-13-yl)styryl)-2,2'-bipyridine (**L1**)¹⁷ was synthesized using a modified procedure of previous references. ¹H NMR and ¹³C NMR spectra were recorded on a Varian Mercury 300 spectrometer. Elemental analyses were performed with a Carlo Erba Instruments CHNS-O EA 1108 analyzer. Mass spectra were recorded on a JEOL JMS-SX102A instrument. The absorption and photoluminescence spectra were recorded on a Perkin-Elmer Lambda 2S UV-visible spectrometer and a Perkin LS fluorescence spectrometer, respectively. Cyclic voltamogram was carried out with a BAS 100B (Bioanalytical System, Inc.). A three electrode system was used and consisted of a

[†]This paper is dedicated to Professor Eun Lee on the occasion of his honourable retirement.

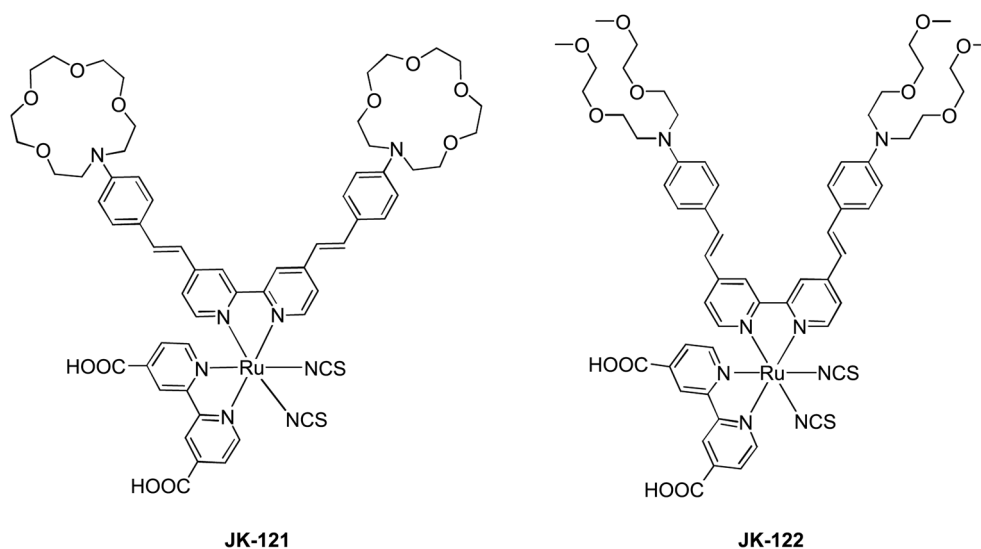


Figure 1. Molecular structure of **JK-121** and **JK-122**.

reference electrode, working electrode, and a platinum wire electrode. Redox potential of dyes on TiO_2 was measured in CH_3CN with 0.1 M $(n\text{-C}_4\text{H}_9)_4\text{N-PF}_6$ with a scan rate between 100 mVs^{-1} (vs. NHE).

Nanosecond Laser Transient Absorption Measurements. Nanosecond transient absorption measurements were carried out by employing the technique of laser flash photolysis. In order to excite the sample solar cells, nanosecond pulse (3.5 ns fwhm) at 504 nm were generated by an H2-Raman shifter from the third harmonic generation (THG, 355 nm) of Q-switched ND:YAG laser (Continuum, Surelite II). A Xenon lamp (ILC Technology, PS 300-1) was focused into the sample solution as the probe light for the transient absorption measurement. Temporal profiles were measured with a monochromator (DongWoo Optron, Monota 500i) equipped with a photomultiplier (Zolix Instruments Co., CR 131) and a digital oscilloscope (Tektronix, TDS-784D). Reported signals were averages of 3000 events.

Fabrication of DSSC. For the preparation of DSSC, a washed FTO (Pilkington, $8 \Omega\text{sq}^{-1}$) glass plate was immersed in 40 mM TiCl_4 aqueous solution as reported by the Grätzel group. The first TiO_2 layer of 7 μm thickness was prepared by screen printing with transparent mesoporous TiO_2 paste (13 nm anatase, Solaronix), and the second opaque layer of 4 μm thickness (400 nm, CCIC) was coated for the purpose of light scattering. The TiO_2 electrodes were immersed into the dyes (**JK-121** and **JK-122**) solution (0.3 mM in acetonitrile: *tert*-butyl alcohol = 1:1 solution) and kept at room temperature for 18 hour. Counter electrodes were prepared by coating with a drop of H_2PtCl_6 solution (2 mg Pt in 1 ml ethanol) on a FTO plate. The electrolyte was then introduced into the cell, which was composed of 0.6 M 3-propyl-1,2-dimethyl imidazolium iodide (DMPImI), 0 M (Electrolyte **A**)/0.05 M (Electrolyte **B**)/0.25 M (Electrolyte **C**)/0.3 M (Electrolyte **D**) lithium perchlorate, 0.1 M iodine and 0.5 M *N*-methylbenzimidazole (NMBI) in acetonitrile.

Characterization of DSSC. The cells were measured

using 1000 W xenon light source, whose power of an AM 1.5 Oriel solar simulator was calibrated by using KG5 filtered Si reference solar cell. The incident photon-to-current conversion efficiency (IPCE) spectra for the cells were measured on an IPCE measuring system (PV Measurements).

Synthesis of Ru(4,4'-bis(4-(1,4,7,10-tetraoxa-13-azacyclopentadecan-13-yl)styryl)-2,2'-bipyridine)(4,4'-dicarboxy-2,2'-bipyridine)(NCS) $_2$ (JK-121**).** A mixture of **L1** (0.18 g, 0.23 mmol) and $[\text{Ru}(\text{Cl})_2(p\text{-cymene})]_2$ (0.069 g, 0.115 mmol) in DMF (40 ml) was heated to 80 $^\circ\text{C}$ for 4 h under nitrogen and then, 4,4'-dicarboxy-2,2'-bipyridine (0.067 g, 0.23 mmol) was added. The reaction mixture was heated to 140 $^\circ\text{C}$ for 4 h under nitrogen and in the dark. NH_4NCS (0.087 g, 1.15 mmol) was then added to the mixture and heating was continued for 4 h. After cooling to room temperature, DMF was evaporated and water (90 ml) was added. The resulting purple solid was filtered and washed with water. The crude complex was dissolved in basic methanol and further purified on a Sephadex LH 20 with methanol as an eluent. The main band was collected and precipitated with dilute acidic methanol to obtain pure **JK-121**. $^1\text{H NMR}$ (300 MHz, $\text{DMSO-}d_6$) δ 9.39 (s, 2H), 9.1 (s, 2H), 8.95 (s, 2H), 8.28 (s, 2H), 7.55-6.55 (m, 16H), 3.68-3.55 (m, 40H). Anal. cal. for $\text{C}_{60}\text{H}_{66}\text{N}_8\text{O}_{12}\text{RuS}_2$: C, 57.36; H, 5.29. Found: C, 57.02; H, 5.21.

Synthesis of *N,N*-Bis(2-(2-methoxyethoxy)ethyl)aniline (A**).** A solution of *N*-phenyldiethanolamine (3 g, 16.6 mmol) in acetonitrile (40 ml) was added dropwise to a suspension of NaH (previously washed twice with hexane to remove the mineral oil, 1.6 g, 60% in NaH, 66.4 mmol) in acetonitrile (30 ml) cooled with an ice-water bath, and then stirred at room temperature for 2 h. A solution of 2-methoxyethyl methanesulfonate (6.38 g, 41.3 mmol) in acetonitrile (30 ml) was then added dropwise at 0 $^\circ\text{C}$. After refluxed overnight, acetonitrile was removed by evaporation, water was added, product was extracted with dichloromethane, dried over

MgSO₄, filtered and evaporated to dryness. Purification was carried out by silica gel column chromatography then, sticky yellow oil product **A** was obtained (3.9 g, 79.4%). ¹H NMR (300 MHz, CDCl₃) δ 7.2 (td, 2H ³J = 7.2), 6.72-6.64 (m, 3H), 3.63-3.51 (m, 16H), 3.35 (s, 9H). ¹³C NMR (75 MHz, CDCl₃) δ 147.2, 128.7, 115.4, 111.1, 71.4, 69.7, 68.1, 58.1, 50.4. Anal. cal. for C₁₆H₂₇NO₄: C, 64.62; H, 9.15. Found: C, 64.21; H, 8.97.

Synthesis of 4-(Bis(2-(2-methoxyethoxy)ethyl)amino) benzaldehyde (B). A solution of **A** (3 g, 10.09 mmol) and hexamethylene-tetramine (1.84 g, 13.13 mmol) in trifluoroacetic acid (5 ml) refluxed for 24 hours. The reaction mixture was cooled to room temperature. Then deionized water/H₂SO₄ (1:1 v/v solution) (20 ml) was added into the reaction mixture solution, and then stirred at room temperature for 30 min. The solution was neutralized by sodium carbonate at pH 7-8. The product was extracted with dichloromethane and the organic phase was washed with deionized water two times then organic phase was dried over MgSO₄, filtered and evaporated to dryness. Purification was carried out by flash silica gel column chromatography, obtaining sticky orange oil product **B** (2.8 g, 85.3%). ¹H NMR (300 MHz, CDCl₃) δ 9.6 (s, 1H), 7.6 (d, 2H ³J = 7.2), 6.67 (d, 2H ³J = 9), 3.6-3.42 (m, 16H), 3.26 (s, 9H). ¹³C NMR (75 MHz, CDCl₃) δ 189.9, 152.5, 131.9, 125, 110.9, 71.7, 70.4, 68, 58.8, 50.8. Anal. cal. for C₁₇H₂₇NO₅: C, 62.75; H, 8.36. Found: C, 62.28; H, 8.28.

Synthesis of 4,4'-(1E,1'E)-2,2'-(2,2'-bipyridine-4,4'-diyl)-bis(ethene-2,1-diyl)bis(N,N-bis(2-(2-methoxyethoxy)ethyl)aniline) (L2). Solid *t*-BuOK (0.33 g, 2.94 mmol) was added to a solution of 4,4'-bis(diethylmethylphosphonate)-2,2'-bipyridine (0.36 g, 0.74 mmol) and **B** (0.6 g, 1.84 mmol) in dry tetrahydrofuran (THF, 20 mL). The resulting mixture was stirred overnight at room temperature under nitrogen. The slurry was then filtered over Celite and the filter cake washed with dichloromethane. Product was extracted with dichloromethane, dried over MgSO₄, filtered and evaporated. Purification was carried out by silica gel column chromatography then, sticky red oil product **L1** was obtained (0.52 g, 70.3%). ¹H NMR (300 MHz, CDCl₃) δ 8.63 (d, 2H ³J = 5.1), 8.48 (s, 2H), 7.45 (d, 2H ³J = 5.2), 7.35-7.3 (m, 4H), 6.93 (d, 2H ³J = 16.5), 6.74 (d, 6H ³J = 8.1), 3.66-3.53 (m, 32H), 3.38 (s, 12H). ¹³C NMR (75 MHz, CDCl₃) δ 156.1, 149.2, 148.1, 147.4, 133.3, 128.7, 115.8, 111.6, 71.4, 69.9, 68.1, 58.3, 50.9. Anal. cal. for C₄₆H₆₂N₄O₈: C, 69.15; H, 7.82. Found: C, 69.48; H, 7.92.

Synthesis of Ru(4,4'-(1E,1'E)-2,2'-(2,2'-bipyridine-4,4'-diyl)bis(ethene-2,1-diyl)bis(N,N-bis(2-(2-methoxyethoxy)ethyl)aniline))(4,4'-dicarboxy-2,2'-bipyridine)(NCS)₂ (JK-122). A mixture of **L2** (0.64 g, 0.8 mmol) and [RuCl₂(*p*-cymene)]₂ (0.24 g, 0.4 mmol) in DMF (40 mL) was heated to 80 °C for 4 h under nitrogen and then, 4,4'-dicarboxy-2,2'-bipyridine (0.24 g, 0.8 mmol) was added. The reaction mixture was heated to 140 °C for 4 h under nitrogen and in the dark. NH₄NCS (0.3 g, 4 mmol) was then added to the mixture and heating was continued for 4 h. After cooling to room temperature, DMF was evaporated and water (90 ml)

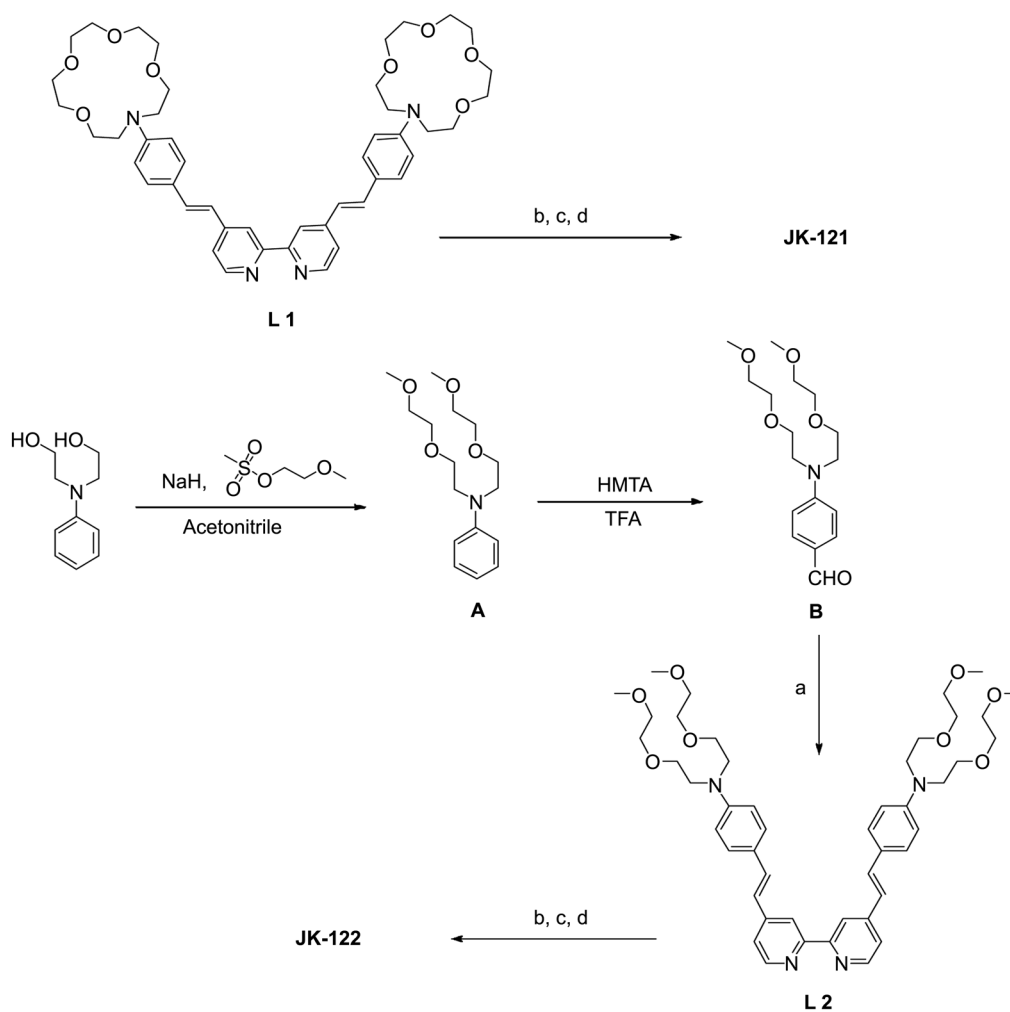
was added. The resulting purple solid was filtered and washed with water. The crude complex was dissolved in basic methanol and further purified on a Sephadex LH 20 with methanol as an eluent. The main band was collected and precipitated with dilute acidic methanol to obtain pure **JK-122**. ¹H NMR (300 MHz, DMSO-*d*₆) δ 9.39 (s, 2H), 9.1 (s, 2H), 8.95 (s, 2H), 8.28 (s, 2H), 7.55-6.55 (m, 16H), 3.65-3.53 (m, 32H), 3.37 (s, 12H). Anal. cal. for C₆₀H₇₀N₈O₁₂RuS₂: C, 57.17; H, 5.60. Found: C, 56.86; H, 5.48.

Result and Discussion

Syntheses and Characterization. The ruthenium sensitizers **JK-121** and **JK-122** were readily prepared by the stepwise synthetic protocol illustrated in Scheme 1. Compound **A** was synthesized using O-alkylation reaction. The phenylamine derivative **A** was converted to its corresponding carbaldehyde **B** according to the Duff reaction. The aldehyde **B**, upon reaction with 4,4'-bis(diethylmethyl-phosphonate)-2,2'-bipyridine in the presence of potassium *tert*-butoxide in THF, produced the ligand **L2**. The reaction of [RuCl₂(*p*-cymene)]₂ complex with **L1** and **L2**, followed by the addition of 4,4'-dicarboxy-2,2'-bipyridine resulted in the heteroleptic dichloro complexes. The chloro complexes react with a large excess of ammonium thiocyanate to afford the ruthenium sensitizers **JK-121** and **JK-122** (Scheme 1).

FT-IR Spectra. ATR-FTIR spectra of sensitizers **JK-121** and **JK-122** grafted on the surface of a TiO₂ film are shown to be a powerful tool to reveal coordination behavior of lithium ion and structural information of **JK-121** and **JK-122**. Fig. 2 shows the typical ATR-FTIR of sensitizer **JK-121** adsorbed on TiO₂ surfaces. The IR spectrum of **JK-121** shows the bands at 1592 and 1381 cm⁻¹, assigning as the asymmetric and symmetric modes of the carboxylate group. These indicate that the two carboxylic acids are involved the attachment of the sensitizer on the surface of TiO₂ in an ester type. The coordinated NCS ligand exhibits a strong absorption at 2101 cm⁻¹, typical of the N-coordinated thiocyanate group. The sensitizer exhibited a characteristic bipyridyl ring stretching mode at 1529 cm⁻¹. The two absorption peaks at 2927 and 2849 cm⁻¹ correspond to the asymmetric and symmetric stretching modes of the CH₂ units of the ethylene oxide unit.

The coordination of sensitizer **JK-121** with the lithium ion was investigated using ATR-FTIR spectroscopy. The **JK-121** sensitizer adsorbed on the TiO₂ film was dipped to a solution of 0.25 M lithium iodide in acetonitrile. In the region of the ν (C-O) stretching mode at 1183 cm⁻¹ in the **L1** of **JK-121**, there is a significant shift to lower energy due to the complexation in **L1** with lithium ion. Upon rinsing the Li⁺-coordinated **JK-121** dye with acetonitrile several times, the original peaks still remain intact. Therefore, the coordination of Li⁺ in the 1,4,7,10-tetraoxa-13-azacyclopentadecane is shown to be strong compared with that of triethyleneoxide methyl ether (TEOME). Similar pattern was shown in the **JK-122** (See S1) incorporated the bis(2-(2-methoxyethoxy)ethyl)-amine group as in the **JK-121**. An analysis of the spectrum in the Fig. 2 indicates that the original ν (C-O)



Scheme 1. Schematic diagram for the synthesis **JK-121** and **JK-122**. Reagents and reaction condition : (a) 4,4'-bis(diethylmethylphosphonate)-2,2'-bipyridine, *t*-BuOK, THF, rt; (b) $[\text{RuCl}_2(p\text{-cymene})]_2$, DMF, 80 °C; (c) 4,4'-dicarboxy-2,2'-bipyridine, DMF, 130 °C; (d) NH_4NCS , DMF, 150 °C.

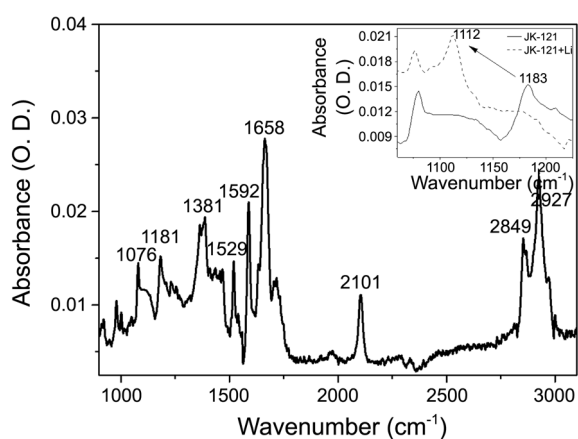


Figure 2. The ATR-FTIR spectrum of the **JK-121** adsorbed on a 6 m mesoporous TiO_2 . The inset shows the difference spectra after the addition of 0.25 M LiI in acetonitrile solution (after 5 min).

peak is diminished by approximately 50% in the presence of the lithium ion. This result suggests that one Li^+ is coordinated to the **JK-121** dye.

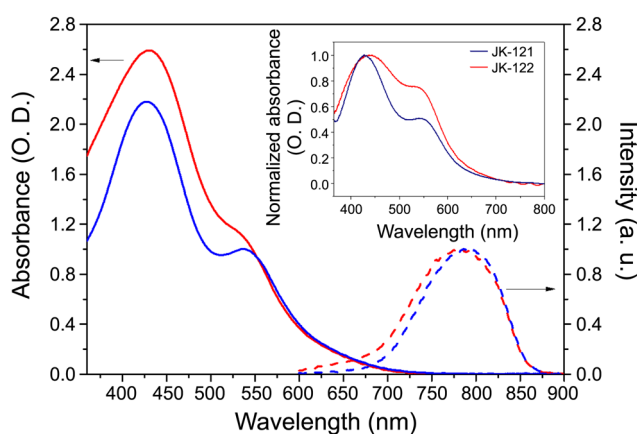


Figure 3. Absorption spectra of **JK-121** (blue solid line) and **JK-122** (red solid line) and emission spectra of **JK-121** (blue dash line) and **JK-122** (red dash line) in 10^{-5} M DMF solution. The inset shows absorption spectra of **JK-121** (blue solid line) and **JK-122** (red solid line) adsorbed on a nanocrystalline TiO_2 film.

Optical Properties. The sensitizers **JK-121** and **JK-122** are weakly soluble in common organic solvents such as

Table 1. Optical, redox, and DSSC performance parameters of dyes

Dye	$\lambda_{\text{abs}}^a/\text{nm}$ ($\epsilon/\text{M}^{-1}\text{cm}^{-1}$)	E_{ox}^b/V	$E_{0,0}^c/\text{V}$	$E_{\text{LUMO}}^d/\text{V}$	J_{sc} (mAcm^{-2})	V_{oc} (V)	F.F	η (%)
JK-121	426 (28,420)	1.05	1.82	-0.77	13.08	0.69	0.77	6.95
	536 (11,060)							
JK-122	429 (42,290)	1.03	1.88	-0.85	10.46	0.67	0.76	5.32
	533 (13,170)							
Z907					10.21	0.65	0.76	5.04

^aAbsorption spectra were measured in DMF. ^bRedox potentials of dyes on TiO_2 were measured in CH_3CN with 0.1 M $(n\text{-C}_4\text{H}_9)_4\text{NPF}_6$ with a scan rate of 100 mVs^{-1} (vs. NHE) ^c $E_{0,0}$ was determined from intersection of absorption and emission spectra in ethanol. ^d E_{LUMO} was calculated by $E_{\text{ox}} - E_{0,0}$.

acetonitrile and dichloromethane. Fig. 3 shows the UV-visible and emission spectra of the **JK-121** and **JK-122** sensitizers in *N,N*-dimethylformamide (DMF) solution, together with the UV-visible spectra of the corresponding sensitizers adsorbed on a TiO_2 film. The absorption spectra of both sensitizers exhibit the characteristic metal-to-ligand charge transfer (MLCT) bands appearing at 426 and 536 nm in **JK-121**, and 429 and 533 nm in **JK-122**, which are about 15 nm red-shifted compared with those of Z907. The molar extinction coefficients of two bands are 28.4×10^3 and $11.0 \times 10^3 \text{ M}^{-1}\text{cm}^{-1}$ in **JK-121** and 42.3×10^3 and $13.1 \times 10^3 \text{ M}^{-1}\text{cm}^{-1}$ in **JK-122**. The enhanced molar extinction coefficients and red shift compared with those of Z907 are attributable to the extension of the π -conjugation of both sensitizers.

The absorption spectra of **JK-121** and **JK-122** on TiO_2 film are broadened due to the interaction of the anchoring group with the surface TiO_2 (Insert in Fig. 2). We observed that the **JK-121** and **JK-122** sensitizers exhibited luminescence maxima at 791 nm and 780 nm, respectively, when they are excited within their MLCT bands at 298 K in an air-equilibrated DMF solution.

Electrochemical Properties. The cyclic voltamogram of **JK-121** and **JK-122** on TiO_2 films in CH_3CN shows quasi-reversible couples at 1.05 and 1.03 V vs NHE, respectively (Table 1). Based on the intersection of absorption and emission spectra, the $E_{0,0}$ transition energy of **JK-121** and **JK-122** is calculated to be 1.82 and 1.88 eV. The excited state redox potentials ($\Phi^{\circ}(\text{S}^+/\text{S}^*)$) of the sensitizers (**JK-121**, -0.77 V; **JK-122**, -0.85 V vs NHE) is negative than the conduction band level of TiO_2 at approximately -0.5 V vs NHE, ensuring that there is an ample driving force for the electron injection into the conduction band of TiO_2 ¹⁹.

Transient Absorbance Spectra. Electron injection from the photo-excited sensitizer is followed by the kinetic competition between recapture of the electrons trapped in the conduction band of the TiO_2 film to the oxidized sensitizer (S^+) or interception of the oxidized sensitizer by the redox couple. Since the kinetic competition between two charge-transfer pathways controls the photovoltaic performance, nanosecond laser experiments were performed to probe the kinetics of these two charge-transfer processes for **JK-121** and **JK-122** dyes. Transient absorbance signals obtained at probe wavelengths of $\lambda > 620 \text{ nm}$ are characteristic of the ligand-to-metal charge-transfer (LMCT) transition of the oxidized Ru(III) complex (S^+) with thiocyanate ligands. In the absence of a redox mediator in acetonitrile, the decay

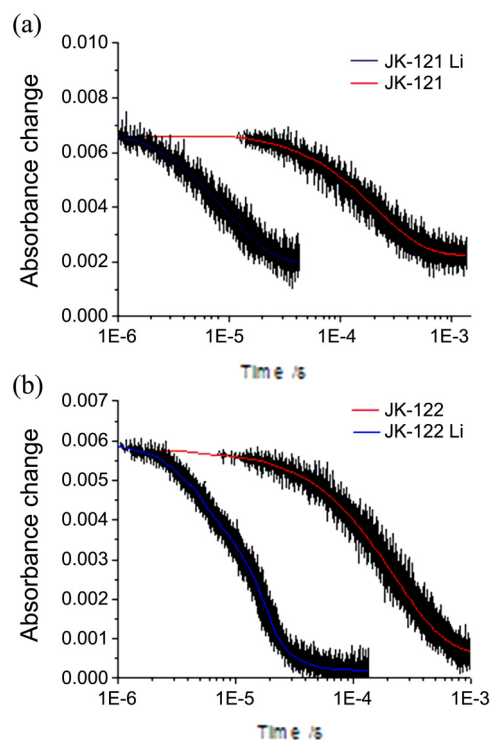


Figure 4. Transient absorbance decay kinetics of the oxidized state of (a) **JK-121** and (b) **JK-122** dye adsorbed on nanocrystalline TiO_2 films in pure acetonitrile (red line), and in the presence of a iodide/triiodide redox couple electrolyte (blue line). Absorbance changes were measured at a probe wavelength of 680 nm upon 504 nm pulsed laser excitation. Signals as shown were obtained by averaging over 3000.

of the absorption signal recorded at 680 nm demonstrates the dynamics of recombination of injected electrons with the oxidized Ru(III) complex. Fig. 4 shows that the kinetics of S^+ transient absorbance decay for the **JK-121** dye has a half-reaction time $t_{1/2} = 280 \mu\text{s}$. The charge recombination kinetic for **JK-121** dye is comparable to what has been reported for the standard N719 dye ($t_{1/2} = 250 \mu\text{s}$)²⁰ and longer than those of ion-coordinating ruthenium sensitizers ($t_{1/2} \sim 200 \mu\text{s}$). In the presence of the iodide/triiodide redox couple, the decay of the oxidized dye signal was significantly accelerated with the half-reaction time $t_{1/2} = 4 \mu\text{s}$. Therefore, the decay of the oxidized dye signal due to regeneration of the **JK-121** dye is much faster than those ($10 \mu\text{s}$) of dyes with the TEOME unit and comparable to that of **K51**²¹ and **K60**¹⁶. Fast dye regeneration of the **JK-121** sensitizer compared to the **K51**

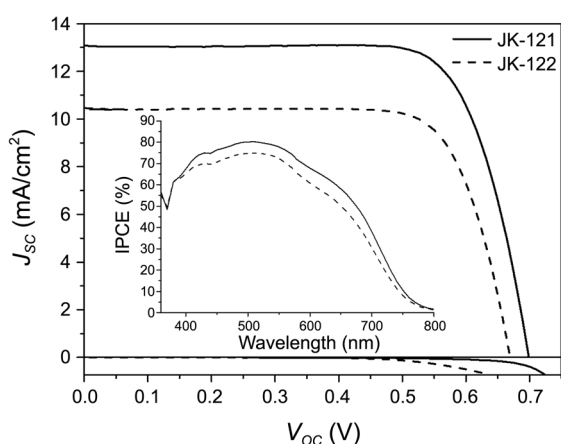


Figure 5. J-V curve and IPCE spectra of **JK-121** (—) and **JK-122** (---).

with TEOME unit and **Z907** implies that more conduction band electron can transport to the electron collector along the TiO₂ surface and thus increase the photocurrent density. The strong coordination of Li⁺ in the 1,4,7,10-tetraoxa-13-azacyclopentadecane of **JK-121** is expected to increase the maximum approach between iodide and the ruthenium center or the thiocyanate ligand and hence increase the dye regeneration rate. A similar behavior was observed for the **JK-122** dye.

Photovoltaic Performances. Fig. 5 shows a photocurrent density-voltage curve for the DSSCs based on the **JK-121** and **JK-122** under standard global AM 1.5 solar conditions. The detailed device parameters are listed in Table 1. The **JK-121** and **JK-122** sensitized cells gave the short-circuit photocurrent density (J_{sc}) of 13.08 and 10.46 mAcm⁻², open circuit voltage (V_{oc}) of 0.69 and 0.67 V and fill factor of 0.77 and 0.76, corresponding to an overall conversion efficiency η of 6.95 and 5.32% respectively. Using similar TiO₂ electrode, electrolyte and measuring conditions the standard sensitizer **Z907** sensitized cell gave a J_{sc} value of 10.21 mAcm⁻², a V_{oc} of 0.65 V and an ff of 0.76, corresponding to a η value of 5.04%. When the photovoltaic performance of **JK-121** and **JK-122** is compared with that of **Z907**, which has a similar absorption spectrum, the efficiency of **JK-121** and **JK-122** is higher than that of **Z907** due to an increase in the J_{sc} and V_{oc} . We attribute the higher values of both parameters based on **JK-121** and **JK-122** to relate to the faster dye generation rate due to the strong coordination of Li⁺ by the 1,4,7,10-tetraoxa-13-azacyclopentadecane unit or bis(2-(2-methoxyethoxy)ethyl)amine. The photocurrent action spectrum of **JK-121** is shown in the insert of Fig. 5. The incident photon-to-current conversion efficiency (IPCE) of **JK-121** exceeds 70% in a broad spectral range 405-595 nm, reaching its maximum of 82% at 510 nm. Integrating the IPCE curve over the solar spectrum of **JK-121** results in a short circuit current of 12.96 mAcm⁻², which is in good agreement with the measured device photocurrent.

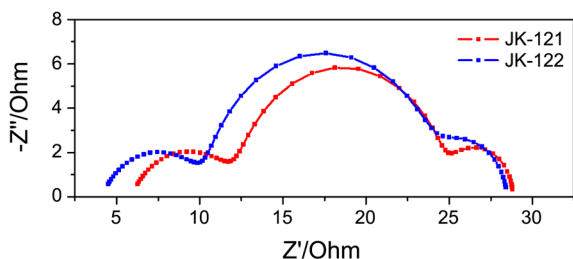
Effect of Li⁺ on Photovoltaic Performance. The influence of various cations added to the electrolyte upon the

photovoltaic performance of DSSCs has been well documented²². Several studies have focused on the utilization of mobile lithium ions to control the interfacial charge transfer, such as tethering of the Li⁺ ion to the surface, pyridine solubilized lithium ions in the organic HTM layer²³, the addition of TEOME units to triarylamine-based molecular conductors, and ruthenium sensitizers tethering TEOME group. We investigated the effect of Li⁺ on the photovoltaic parameters of the DSSCs with **JK-121** and **JK-122** bearing strong coordinating groups. Table 2 shows the influence of Li⁺ concentration upon the short-circuit current and the open-circuit voltage using **JK-121** sensitizer. With the addition of Li⁺ (50 mM) to the electrolyte **A**, the photocurrent increases from 13.08 to 14.32 mAcm⁻² and the voltage decreases from 0.692 to 0.677 V. The stepwise addition of Li⁺ (250 and 300 mM) to the electrolyte **A** causes a slight increase in the photo-current density, with a small decrease in the open circuit voltage. This observation can be explained by a substantial red-shift and broad metal-to-ligand charge transfer (MLCT) peaks when the sensitizer on TiO₂ film was coordinated with Li⁺ ion (See Supporting Information Figure S4). Therefore, the device exhibits small changes in the power conversion efficiency η upon an incremental addition of Li⁺. The observation can be rationalized in terms of the coordination of Li⁺ to an ion-solvating group by preventing Li⁺ from contacting the surface of TiO₂. We also investigated the effect of Li⁺ in the electrolyte with **JK-121** and **JK-122**. When the lithium salt (0.25M LiClO₄) was added to the electrolyte, the V_{oc} of **JK-121** and **JK-122** was dropped to 27 mV and 18 mV, respectively. Under the same condition the V_{oc} of **K60** was dropped to 58 mV¹⁶. The result shows that the sensitizers **JK-121** and **JK-122** are strongly coordinated to the Li⁺ salt compared to **K60**. As the lithium ion has a significant effect upon controlling the interfacial electron transfer reactions in solid-state electrolyte, we extended our studies to such devices using 2,2',7,7'-tetrakis (*N,N*-dimethoxyphenylamine)-9,9'-spirobifluorene (OMeTAD) as a hole conductor. We used lithium triflamide (Li[CF₃SO₂]₂N)²⁴ as a lithium ion source. The **JK-121** sensitized solid-state cell in the presence of Li⁺ (20 mM in chlorobenzene) gave the short-circuit photocurrent density (J_{sc}) of 9.54 mAcm⁻², open-circuit voltage (V_{oc}) of 0.698 V and a fill factor of 0.39, affording an overall conversion efficiency η of 2.59%. We find that the same device in the absence of Li⁺ resulted in a poor performance (η = 1.85%). It is apparent that the addition of Li⁺ in a hole conductor resulted in a 30% improvement in efficiency due to a strong coordination of Li⁺ to an ion-complexing unit in **JK-121**. Such a Li⁺ coordination results in a retardation of the interfacial recombination reaction due to electrostatic screening of the photo-injected electron from the hole transfer material (HTM) cation.

Impedance Spectra. The ac impedances of the cells were measured under illumination conditions (Fig. 6). The measurement showed three semicircles in the Nyquist diagram. Under the illumination (100 mWcm⁻², open-circuit voltage conditions), the radius of the intermediate frequency

Table 2. Photovoltaic performance data of **JK-121** containing different lithium cation concentration in the electrolyte

Dye	Electrolyte	Conc. of LiClO ₄	J _{sc} (mAcm ⁻²)	V _{oc} (V)	F.F	η (%)
JK-121	A	0 M	13.08	0.692	0.77	6.95
	B	0.05 M	14.32	0.677	0.77	7.46
	C	0.25 M	14.52	0.665	0.75	7.24
	D	0.3 M	14.77	0.663	0.73	7.15

**Figure 6.** Electrochemical impedance spectra (nyquist plot) measured under the illumination (100 mWcm⁻²) for the devices employing different dyes (Red : **JK-121**, Blue : **JK-122**).

semicircle in the Nyquist plot decrease in the order of **JK-122** (12.96 Ω) > **JK-121** (11.65 Ω), indicating the improved electron generation and transport. This result corresponds well to that of the short-circuit current shown in Table 1.

Conclusion

Two new ion coordinating ruthenium complexes [Ru(dcbpy)(L)(NCS)₂, where dcbpy is 4,4'-dicarboxylic acid-2,2'-bipyridine and L is 1,4,7,10-tetraoxa-13-azacyclopenta-decane or bis(2-(2-methoxyethoxy)ethyl)amine] were synthesized. The device based on the sensitizer **JK-121** in the liquid electrolyte gave an overall conversion efficiency of 6.95%. The lithium ion has a significant effect upon the photovoltaic performance particularly in solid-state electrolyte. The **JK-121** sensitized solid-state cell in the presence of Li⁺ gave an overall conversion efficiency of 2.59%, which showed a 30% improvement in efficiency compared with the device in the absence of Li⁺ due to a retardation of the interfacial recombination. FTIR and nanosecond laser experiment studies proved the coordination effect of the **JK-121** and Li⁺.

Acknowledgments. We are grateful to the Korea University Research Program (2010).

References

- (a) O'Regen, B.; Grätzel, M. *Nature* **1991**, 353, 737. (b) Hagfeldt, A.; Grätzel, M. *Chem. Rev.* **1995**, 95, 49. (c) Hagfeldt, A.; Grätzel, M. *Acc. Chem. Res.* **2000**, 33, 269.
- (a) Nazeeruddin, M. K.; De Angelis, F.; Fantacci, S.; Selloni, A.; Viscardi, G.; Liska, P.; Ito, S.; Takeru, B.; Grätzel, M. *J. Am. Chem. Soc.* **2005**, 127, 16835. (b) Chiba, Y.; Islam, A.; Watanabe, Y.; Komiyama, R.; Koide, N.; Han, L. *Jpn. J. Appl. Phys. Part 2* **2006**, 45, L638. (c) Gao, F.; Wang, Y.; Shi, D.; Zhang, J.; Wang, M.; Jing, X.; Humphry-Baker, R.; Wang, P.; Zakeeruddin, S. M.; Grätzel, M. *J. Am. Chem. Soc.* **2008**, 130, 10720.
- (a) Palomares, E.; Clifford, J. N.; Haque, S. A.; Lutz, T.; Durrant, J. R. *J. Am. Chem. Soc.* **2003**, 125, 475. (b) Clifford, J. N.; Yahiolglu, G.; Milgrom, L.; R.; Durrant, J. R. *Chem. Commun.* **2002**, 1260. (c) Palomares, E.; Clifford, J. N.; Haque, S. A.; Lutz, T.; Durrant, J. R. *Chem. Commun.* **2002**, 1464.
- (a) Brown, T. M.; Friend, R. H.; Millard, I. S.; Lacey, D. J.; Burroughes, J. H.; Cacialli, F. *Appl. Phys. Lett.* **2001**, 79, 174. (b) Palomares, E.; Clifford, J. N.; Haque, S. A.; Lutz, T.; Durrant, J. R. *J. Am. Chem. Soc.* **2003**, 125, 574. (c) Kruger, J.; Bach, V.; Grätzel, M. *Adv. Mater.* **2000**, 12, 447.
- Handa, S.; Haque, S. A.; Durrant, J. R. *Adv. Funct. Mater.* **2007**, 17, 2878.
- (a) Satoh, N.; Nakashima, T.; Yamamoto, K. *J. Am. Chem. Soc.* **2005**, 127, 13030. (b) Nakashima, T.; Satoh, N.; Albrecht, K.; Yamamoto, K. *Chem. Mater.* **2008**, 20, 2538.
- (a) Jiang, K. -J.; Masaki, N.; Xia, J. -B.; Noda, S.; Yanagida, S. *Chem. Commun.* **2006**, 2460. (b) Gao, F.; Wang, Y.; Zhang, J.; Shi, D.; Wang, M.; Humphry-Baker, R.; Wang, P.; Zakeeruddin, S. M.; Grätzel, M. *Chem. Commun.* **2008**, 2635. (c) Chen, C. -Y.; Wu, S. -J.; Wu, C. -G.; Chen, J. -G.; Ho, K. -C. *Angew. Chem. Int. Ed.* **2006**, 45, 5822. (d) Koumura, N.; Wang, Z. -S.; Mori, S.; Miyashita, M.; Suzuki, E.; Hara, K. *J. Am. Chem. Soc.* **2006**, 128, 14256. (e) Choi, H.; Baik, C.; Kang, S. O.; Ko, J.; Kang, M. -S.; Nazeeruddin, M. K.; Grätzel, M. *Angew. Chem. Int. Ed.* **2008**, 47, 327.
- (a) Wang, P.; Zakeeruddin, S. M.; Humphry-Baker, R.; Grätzel, M. *Chem. Mater.* **2004**, 16, 2694. (b) Wang, P.; Zakeeruddin, S. M.; Humphry-Baker, R.; Moser, J. E.; Grätzel, M. *Adv. Mater.* **2003**, 15, 2101.
- (a) Nakade, S.; Kambe, S.; Kitamura, T.; Wada, Y.; Yanagida, S. *J. Phys. Chem. B* **2001**, 105, 9150. (b) Lindström, H.; Södergren, S.; Solbrand, A.; Rensmo, H.; Hjelm, J.; Hagfeldt, A.; Lindquist, S. -E. *J. Phys. Chem. B* **1997**, 101, 7717.
- Park, T.; Haque, S. A.; Potter, R. J.; Holmes, A. B.; Durrant, J. R. *Chem. Commun.* **2003**, 2878.
- Haque, S. A.; Park, T.; Xu, C.; Koops, S.; Schulte, N.; Potter, R. J.; Holmes, A. B.; Durrant, J. R. *Adv. Funct. Mater.* **2004**, 14, 435.
- Hirata, N.; Kroeze, J. E.; Park, T.; Jones, D.; Haque, S. A.; Holmes, A. B.; Durrant, J. R. *Chem. Commun.* **2006**, 535.
- Kroeze, J. E.; Hirata, N.; Schmidt-Mende, L.; Orizu, C.; Ogier, S. D.; Carr, K.; Grätzel, M.; Durrant, J. R. *Adv. Funct. Mater.* **2006**, 16, 1832.
- Snaith, H. J.; Zakeeruddin, S. M.; Schmidt-Mende, L.; Klein, C.; Grätzel, M. *Angew. Chem. Int. Ed.* **2005**, 44, 6413.
- Kuang, D.; Klein, C.; Snaith, H. J.; Moser, J. -E.; Humphry-Baker, R.; Comte, P.; Zakeeruddin, S. M.; Grätzel, M. *Nano Lett.* **2006**, 6, 769.
- Kuang, D.; Klein, C.; Ito, S.; Moser, J. -E.; Humphry-Baker, R.; Zakeeruddin, S. M.; Grätzel, M. *Adv. Funct. Mater.* **2007**, 17, 154.
- Beer, P. D.; Kocian, O.; Mortimer, R. J.; Ridgway, C. *J. Chem. Soc. Chem. Commun.* **1991**, 1460.
- Ros-Lis, J. V.; Garcia, B.; Jiménez, D.; M-Manez, R.; Sancenón, F.; Soto, J.; Gonzalez, F.; Valdecabres, M. C. *J. Am. Chem. Soc.* **2004**, 126, 4064.
- (a) Bond, A. M.; Deacon, G. B.; Howitt, J.; MacFarlane, D. R.; Spiccia, L.; Wolfbauer, G. *J. Electrochem. Soc.* **1999**, 146, 648. (b) Wang, P.; Zakeeruddin, S. M.; Moser, J. -E.; Grätzel, M. *J. Phys.*

- Chem. B* **2003**, *107*, 13280.
20. Pelet, S.; Moser, J. E.; Grätzel, M. *J. Phys. Chem. B* **2000**, *104*, 1791.
21. Kuang, D.; Klein, C.; Snaith, H. J.; Moser, J.-E.; Humphry-Baker, R.; Comte, P.; Zakeerudin, S. M.; Grätzel, M. *Nano. Lett.* **2006**, *6*, 769.
22. Zahan, A.; Meier, A.; Gregg, B. A. *J. Phys. Chem. B* **1997**, *101*, 7985.
23. Kruger, J.; Plass, R.; Cevey, L.; Piccirelli, M.; Grätzel, M.; Bach, U. *Appl. Phys. Lett.* **2001**, *79*, 2085.
24. Schmidt-Mende, L.; Zakeeruddin, S. M.; Grätzel, M. *Appl. Phys. Lett.* **2005**, *86*, 013504
-